Proc. R. Soc. Lond. A **370**, 459–484 (1980)
Printed in Great Britain

On the Weierstrass–Mandelbrot fractal function

BY M. V. BERRY AND Z. V. LEWIS
H.H. Wills Physics Laboratory, Tyndall Avenue, Bristol, BS8 1TL, U.K.

(*Communicated by J. F. Nye, F.R.S. – Received 5 July* 1979)

The function

$$W(t) \equiv \sum_{n=-\infty}^{\infty} \frac{[(1-e^{i\gamma^n t})e^{i\phi_n}]}{\gamma^{(2-D)n}} \quad (1 < D < 2, \quad \gamma > 1, \quad \phi_n = \text{arbitrary phases}),$$

is continuous but non-differentiable and possesses no scale. The graph of Re W or Im W has Hausdorff–Besicovitch (fractal) dimension D. Choosing $\phi_n = \mu n$ gives a deterministic W the scaling properties of which can be studied analytically in terms of a representation obtained by using the Poisson summation formula. Choosing ϕ_n random gives a stochastic W whose increments $W(t+\tau) - W(t)$ are statistically stationary, with a mean square which, as a function of τ, is smooth if $1.0 < D < 1.5$ and fractal if $1.5 < D < 2.0$. The properties of W are illustrated by computed graphs for several values of D (including some 'marginal' cases $D = 1$ where the series for W converges) and several values of γ, with deterministic and random ϕ_n, for $0 \leqslant t \leqslant 1$ and the magnified range $0.30 \leqslant t \leqslant 0.31$. The Weierstrass spectrum γ^n can be generated by the energy levels of the quantum-mechanical potential $-A/x^2$, where $A = \frac{1}{4} + 4\pi^2/\ln^2\gamma$.

1. INTRODUCTION

Mandelbrot (1977) discusses the celebrated function devised by Weierstrass in 1872, which although continuous everywhere is differentiable nowhere. He points out that the Weierstrass function is a fractal, in the sense that its graph is a curve whose Hausdorff-Besicovitch dimension exceeds unity. As the function's fractality implies, it has no smallest scale. But it does have a largest scale, and this might be a disadvantage when using it to model fractal phenomena. Therefore Mandelbrot proposes the following extension of the Weierstrass function, which has no scale at all:

$$W(t) \equiv \sum_{n=-\infty}^{\infty} \frac{(1-e^{i\gamma^n t})e^{i\phi_n}}{\gamma^{(2-D)n}} \quad (1 < D < 2, \quad \gamma > 1, \quad \phi_n = \text{arbitrary phases}). \quad (1)$$

D is taken to be the Hausdorff–Besicovitch (fractal) dimension of the graph of $W(t)$, by which we mean, since W is complex, the graph of Re W or Im W. γ is a parameter, and the phases ϕ_n can be chosen to make W exhibit deterministic or stochastic behaviour. The frequencies γ^n form a 'Weierstrass spectrum', spanning the range zero to infinity in geometric progression; this is the sense in which W possesses no scale. With the indicated restrictions on γ and D, the series for W converges but the series for dW/dt does not.

We shall call W the 'Weierstrass–Mandelbrot function'. In view of its mathematical importance and potential applicability, W deserves detailed analytical and computational study. This paper is a first step in that direction.

At the outset we admit to a difficulty: so far as we know, there does not yet exist a proof that D is in fact the fractal dimension of W. We do, however, strongly believe that this is the case, for theoretical and 'experimental' reasons to be given in § 4 after the necessary analysis has been developed; until then we simply assume it.

The fractal nature of W implies that repeated magnification of its graph reveals ever-finer levels of detail. Such behaviour contrasts sharply with that of a differentiable function, whose graph tends to a straight line when magnified. The levels of detail are self-similar under an affine scaling in which the t axis is stretched by a factor γ and the W axis by γ^{2-D}. In the deterministic case, discussed in § 2, ϕ_n is chosen to be a linear function of n, and the origin $t = 0$ plays a crucial role in the scaling, a fact explained by Poisson transformation of the series (1). In the stochastic case, discussed in § 3, $\{\phi_n\}$ is chosen to be a set of random numbers, and the scaling is embodied in the mean square increment of W between two points. These two kinds of scaling are illustrated by graphs of $W(t)$ obtained by numerical computation from (1).

Three special values of D are particularly interesting. For the 'Brownian' fractal, $D = 1.5$ and $W(t)$ is a model for the distance travelled along the W axis in time t by a particle moving in infinitesimal steps which are equally likely to be backwards or forwards. For the 'extreme' fractal, $D \to 2$ and $W(t)$, whose graph is almost area-filling, is a model for '$1/f$ noise' (Mandelbrot 1977; Press 1978); our computations in this case are for $D = 1.99$. For the 'marginal' fractal, $D = 1$ and $W(t)$ is a model for a section through a conjectured subglacial landscape (Nye 1970) self-similar under equal magnifications in the W and t directions; when $D = 1$ the convergence of the series (1) is determined by the behaviour of ϕ_n as $n \to -\infty$, whereas the function's fractal nature is determined by ϕ_n as $n \to +\infty$; for our computations we chose $\{\phi_n\}$ for which (1) does converge.

In addition to $D = 1$, 1.5 and 1.99 we also studied $D = 1.2$ and 1.8. For each of these values, we computed graphs of $W(t)$ for $\gamma = 1.2$, 1.5 and 5 over the ranges $0 \leqslant t \leqslant 1$ and the hundredfold magnification $0.30 \leqslant t \leqslant 0.31$. This gave thirty different types of graph. There were four versions of each type, corresponding to three deterministic sets and one random set $\{\phi_n\}$, excepting those cases for $D = 1$ where the series (1) does not converge. Limitations of space restrict us to showing only an illustrative selection of all these graphs. Details of computational procedures, and the overcoming of a difficulty arising from the fact that W has a Weierstrass spectrum, are described in the appendix.

The frequencies in Fourier series form an arithmetic progression, and such linear spectra are familiar from elementary eigenvalue problems like the vibrating string, the harmonic oscillator and the components of the angular momentum operator. By contrast, the Weierstrass spectrum of $W(t)$ seems not to have been discussed before. In § 5 we show how it can be generated naturally by a quantum-mechanical Hamiltonian whose potential is weakly singular.

2. Deterministic functions

These are given by (1) with the phases chosen as

$$\phi_n = \mu n. \tag{2}$$

W can now easily be shown to obey the affine scaling law

$$W(\gamma t) = \mathrm{e}^{-\mathrm{i}\mu}\gamma^{2-D}\,W(t). \tag{3}$$

This implies that the whole function W can be reconstructed from its values in the range $t_0 \leqslant t < \gamma t_0$; for example, W in the ranges $\gamma t_0 \leqslant t < \gamma^2 t_0$ and $\gamma^{-1} t_0 \leqslant t < t_0$ are magnified and diminished versions, respectively, of W in the range $t_0 \leqslant t < \gamma t_0$.

As a first illustration of this scaling we consider the cosine series

$$C(t) \equiv \operatorname{Re} W(t)_{(\mu=0)} = \sum_{n=-\infty}^{\infty} \frac{(1-\cos\gamma^n t)}{\gamma^{(2-D)n}}, \tag{4}$$

which also converges for the marginal case $D = 1$. $C(t)$ is never negative. Figures 1 (*a–e*) show $C(t)$ for $D = 1$, 1.2, 1.5, 1.8, and 1.99 with $\gamma = 1.5$, for $0 \leqslant t \leqslant 1$. It is clear how the form of $C(t)$ near any point t_0 is repeated, magnified and revealing more detail, near γt_0, $\gamma^2 t_0$, etc.

As a second illustration we consider the alternating-sign sine series

$$A(t) \equiv -\operatorname{Im} W(t)_{(\mu=\pi)} = \sum_{n=-\infty}^{\infty} \frac{(-1)^n \sin\gamma^n t}{\gamma^{(2-D)n}}, \tag{5}$$

which does not converge when $D = 1$. $A(t)$ must change sign infinitely often, because (3) implies $A(\gamma t)/A(t) < 0$. Figures 2 (*a–d*) show $A(t)$ for $D = 1.2$, 1.5, 1.8 and 1.99 with $\gamma = 1.5$, for $0 \leqslant t \leqslant 1$. The repetition and resolution of features at t_0, γt_0, $\gamma^2 t_0$ etc. is again obvious.

The graphs of $C(t)$ (figure 1) and $A(t)$ (figure 2) look rather different, although they both show fractal curves with the same D. This is because the range of t depicted includes the origin and so contains infinitely many γ-periods exemplifying the scaling (3), which implies very different behaviour for functions with $\mu = 0$ and $\mu = \pi$. To demonstrate the respects in which $C(t)$ and A(t) are similar, it is necessary to look in detail at a range of t that does not include the origin and which is smaller than a γ-period. This is shown on figures 3 *a–d*, which are magnifications of figures 1 *c*, 1 *d*, 2 *b* and 2 *c* respectively, displaying the range $0.3 \leqslant t \leqslant 0.31$. The resemblance between functions with the same fractal dimension is now much clearer.

The scaling law (3) does not imply that $W(t)$ is a fractal, because it is satisfied by smooth functions of the form

$$f_m(t) = t^{2-D}\exp\left[-\mathrm{i}(\mu + 2\pi m)\ln t/\ln\gamma\right], \tag{6}$$

where m is any integer. These functions can be combined into an alternative series for $W(t)$ which will of course have the property, not shared by (1), that the individual

terms all obey (3). To obtain this new series, we transform the sum over n in (1) by the Poisson formula (Lighthill 1958), and obtain

$$W(t) = \sum_{m=-\infty}^{\infty} \int_{-\infty}^{\infty} \mathrm{d}n \frac{(1-\mathrm{e}^{\mathrm{i}\gamma^n t})\,\mathrm{e}^{\mathrm{i}(\mu+2\pi m)n}}{\gamma^{(2-D)n}}. \tag{7}$$

After integrating by parts, the terms in this series can be expressed as Γ functions (Abramowitz & Stegun 1964), with the result

$$W(t) = \frac{\mathrm{e}^{\frac{1}{2}\mathrm{i}\pi D}\,\mathrm{e}^{-\mu\pi/2\ln\gamma}}{\ln\gamma} \sum_{m=-\infty}^{+\infty} f_m(t)\,\mathrm{e}^{-\pi m^2/\ln\gamma}\,\Gamma\left(D-2+\frac{\mathrm{i}(\mu+2\pi m)}{\ln\gamma}\right). \tag{8}$$

Application of Stirling's formula shows that the terms decay as $\exp(-2m\pi^2/\ln\gamma)$ as $m\to+\infty$ and as $|m|^{-(\frac{5}{2}-D)}\times\exp(\mathrm{i}m\times\text{constant})$ as $m\to-\infty$; therefore the series is convergent. The convergence is fastest when $\gamma\to 1$, in contrast to (1) whose convergence is fastest when $\gamma\to\infty$.

An immediate application of (8) explains the trends of the curves on figures 1 and 2, as given by the most slowly varying contributions to $W(t)$. If we try to identify these in equation (1), we find only the zero-frequency terms $n\to-\infty$, whose value is hard to estimate. From (8) and (6), it is obvious that the most slowly-varying contributions correspond to $m=0$ ($\mu=0$) and $m=0,\,-1$ ($\mu=\pi$). In the case of $C(t)$ (equation (4)), the trend is

$$C(t) \approx \frac{t^{2-D}\,\Gamma(D-1)\cos\frac{1}{2}\pi(2-D)}{(2-D)\ln\gamma}. \tag{9}$$

In the case of $A(t)$ (equation (5)), the term $m=-1$ dominates the term $m=0$ because of the exponential in (8), giving the trend

$$A(t) \approx \frac{-t^{2-D}\,\mathrm{e}^{\pi^2/2\ln\gamma}}{\ln\gamma}\,\mathrm{Im}\left\{\mathrm{e}^{\mathrm{i}\pi(\frac{1}{2}D+\ln t/\ln\gamma)}\,\Gamma\left(D-2-\frac{\mathrm{i}\pi}{\ln\gamma}\right)\right\}. \tag{10}$$

If $\pi/\ln\gamma$ is sufficiently large this can be simplified by using Stirling's formula, to give, after some calculation, the trend

$$A(t) \approx \left(\frac{2}{\ln\gamma}\right)^{\frac{1}{2}}\left(\frac{t\ln\gamma}{\pi}\right)^{2-D}\sin\left[\frac{\pi}{\ln\gamma}\ln\left(\frac{\mathrm{e}t\ln\gamma}{\pi}\right)+\frac{\pi}{4}\right]. \tag{11}$$

The trends (9) and (11) are plotted as the smooth curves on figures 1 and 2 respectively; evidently they represent the overall behaviour of $C(t)$ and $A(t)$ very well.

All the graphs on figures 1—3 were computed with $\gamma=1.5$. The effect of varying γ can be seen on figure 4. Figures 4(a, b) show $C(t)$ ($0\leqslant t\leqslant 1$) for $\gamma=1.2$ and 5 respectively, with $D=1.5$; they should be compared with figure 1c. As expected, increasing γ separates the scales of variation of the function. Figures 4(c, d) are similar to figures 4(a, b) but with the range $0.3\leqslant t\leqslant 0.31$, and should therefore be compared with figure 3a. For these magnified graphs, the effect of varying γ is much less pronounced; the fractal dimension shared by the graphs is relatively more important (a point we shall take up again in §4).

3. Stochastic functions

Let $\{\phi_n\}$ in (1) be a set of random numbers on the range 0 to 2π. Then $W(t)$ is the sum of infinitely many contributions with random phases and so is a Gaussian random function (Rice 1944, 1945). Figures 5(*a–e*) show some of these random fractal functions: Re $W(t)$ $(0 \leqslant t \leqslant 1)$ for $D = 1$, 1.2, 1.5, 1.8 and 1.99 with $\gamma = 1.5$. In the case $D = 1$, the convergence of (1) is assured by choosing $\phi_n = a_n \pi$, where the a_n are a random sequence of zeros and ones.

Each such $W(t)$ is a member of the ensemble of random functions generated by all possible sets $\{\phi_n\}$. Included in this ensemble as a subclass of zero measure are the deterministic functions discussed in § 2. No other functions W satisfy the scaling (3), so that in general the origin $t = 0$ is not the source of γ-periodicity; this is obvious from figure 5, especially in comparison with figures 1 and 2.

Figures 6(*a–e*) show hundred-fold magnifications of figures 5(*a–e*), i.e. Re $W(t)$ $(0.30 \leqslant t \leqslant 0.31)$. The similarity is so striking that if the axes were not labelled it would be impossible to decide which graphs were the originals and which were the enlargements.

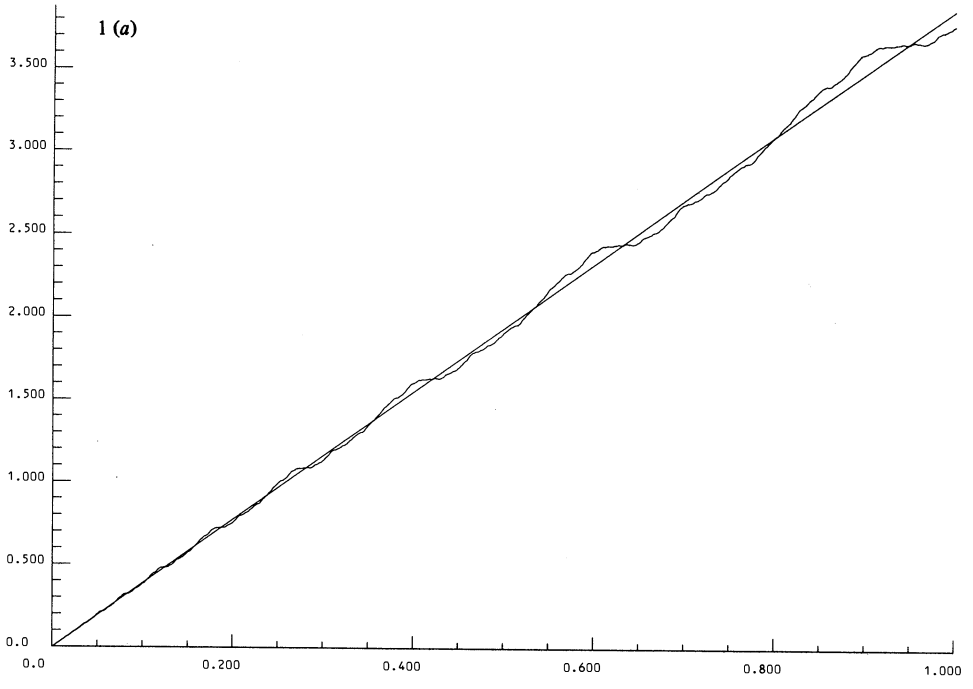

Figure 1 (*a*) For legend see page 465.

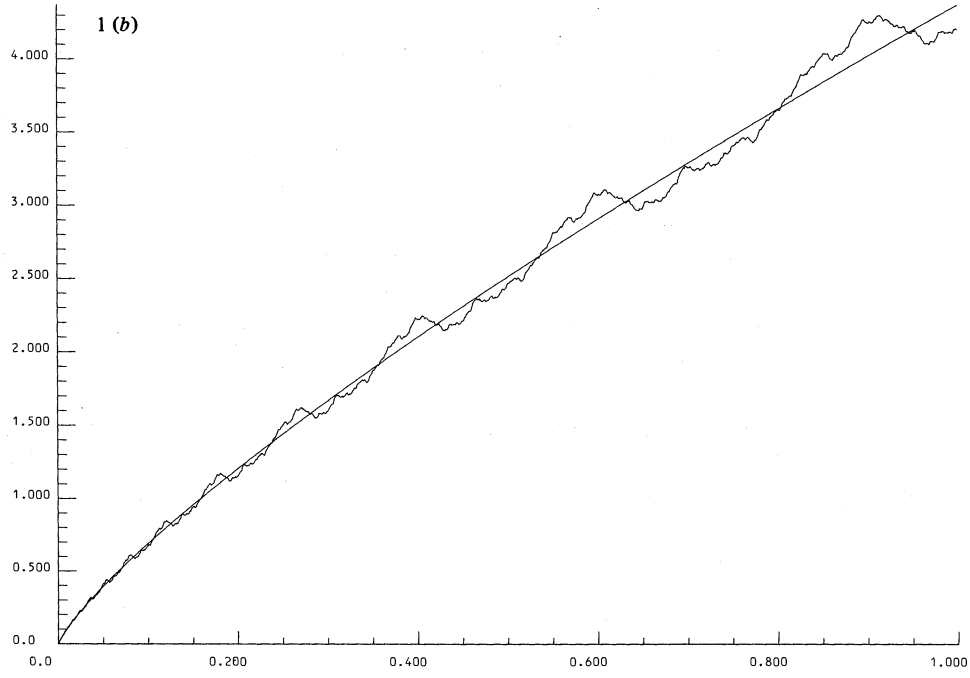

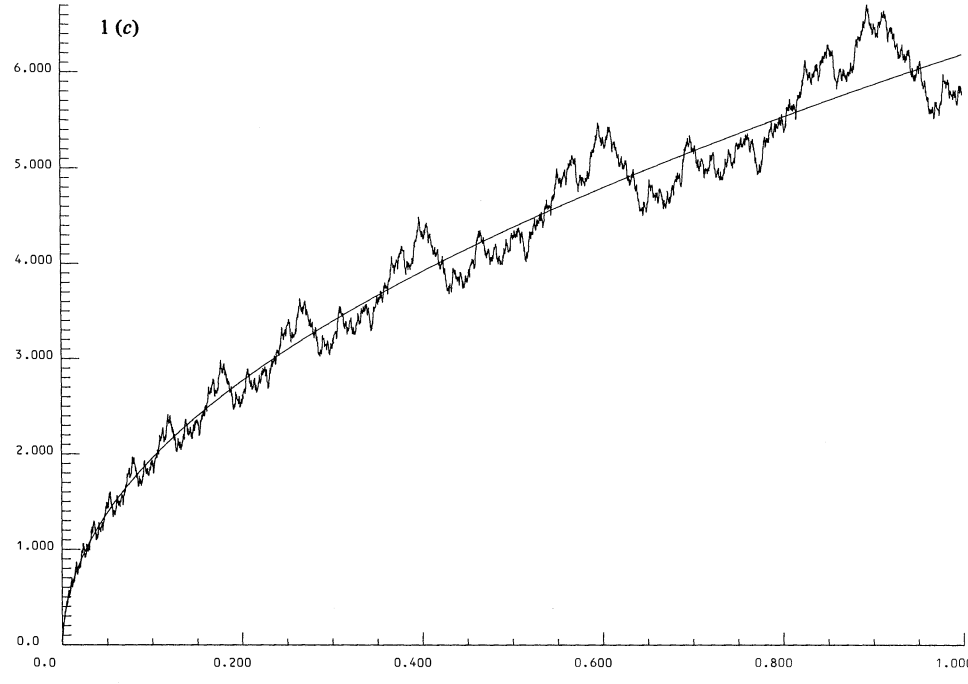

FIGURE 1 (*b*), (*c*) For legend see page 464.

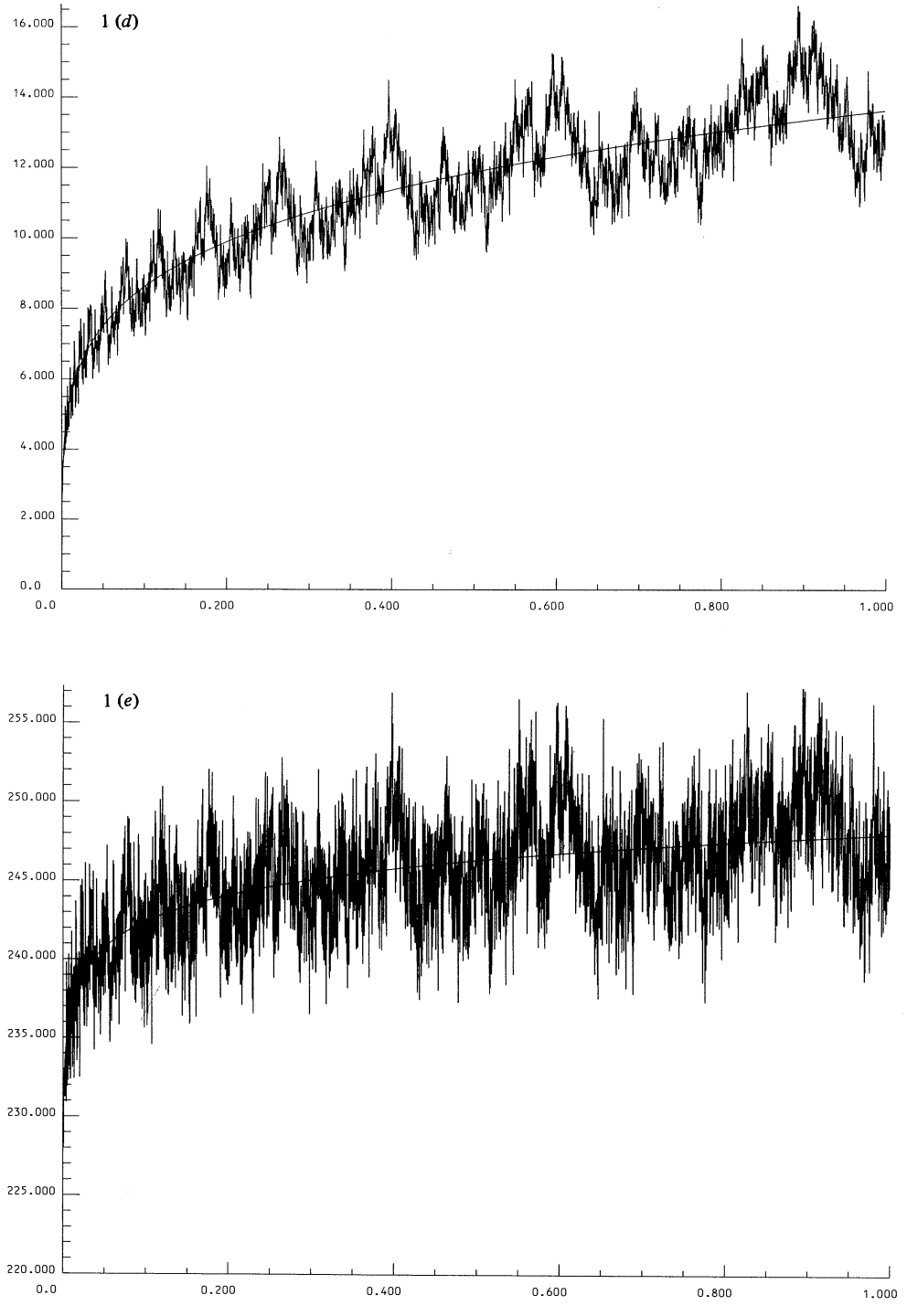

FIGURE 1. Weierstrass–Mandelbrot cosine fractal function $C(t)$, range $0 \leqslant t \leqslant 1$, $\gamma = 1.5$: (*a*) $D = 1$; (*b*) $D = 1.2$; (*c*) $D = 1.5$; (*d*) $D = 1.8$; (*e*) $D = 1.99$ (note change of origin).

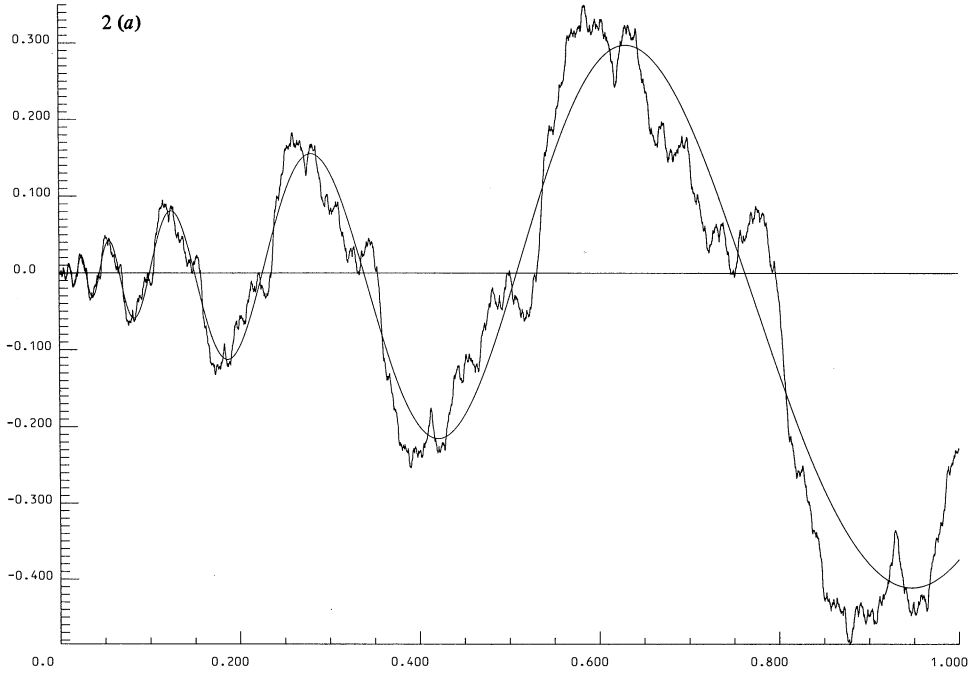

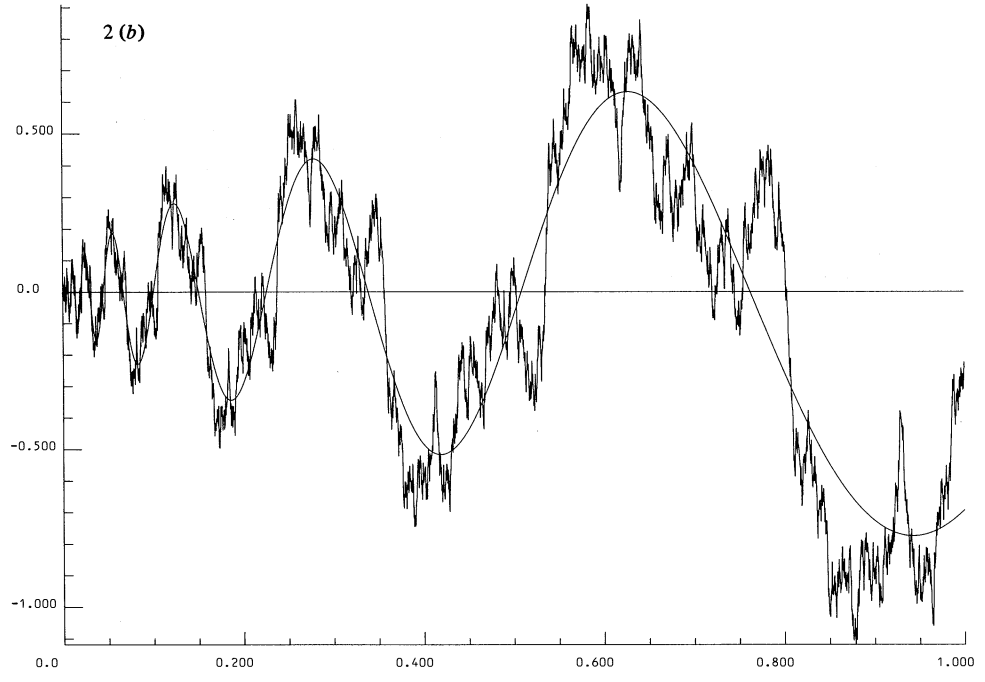

FIGURE 2 (*a*), (*b*) For legend see page 467.

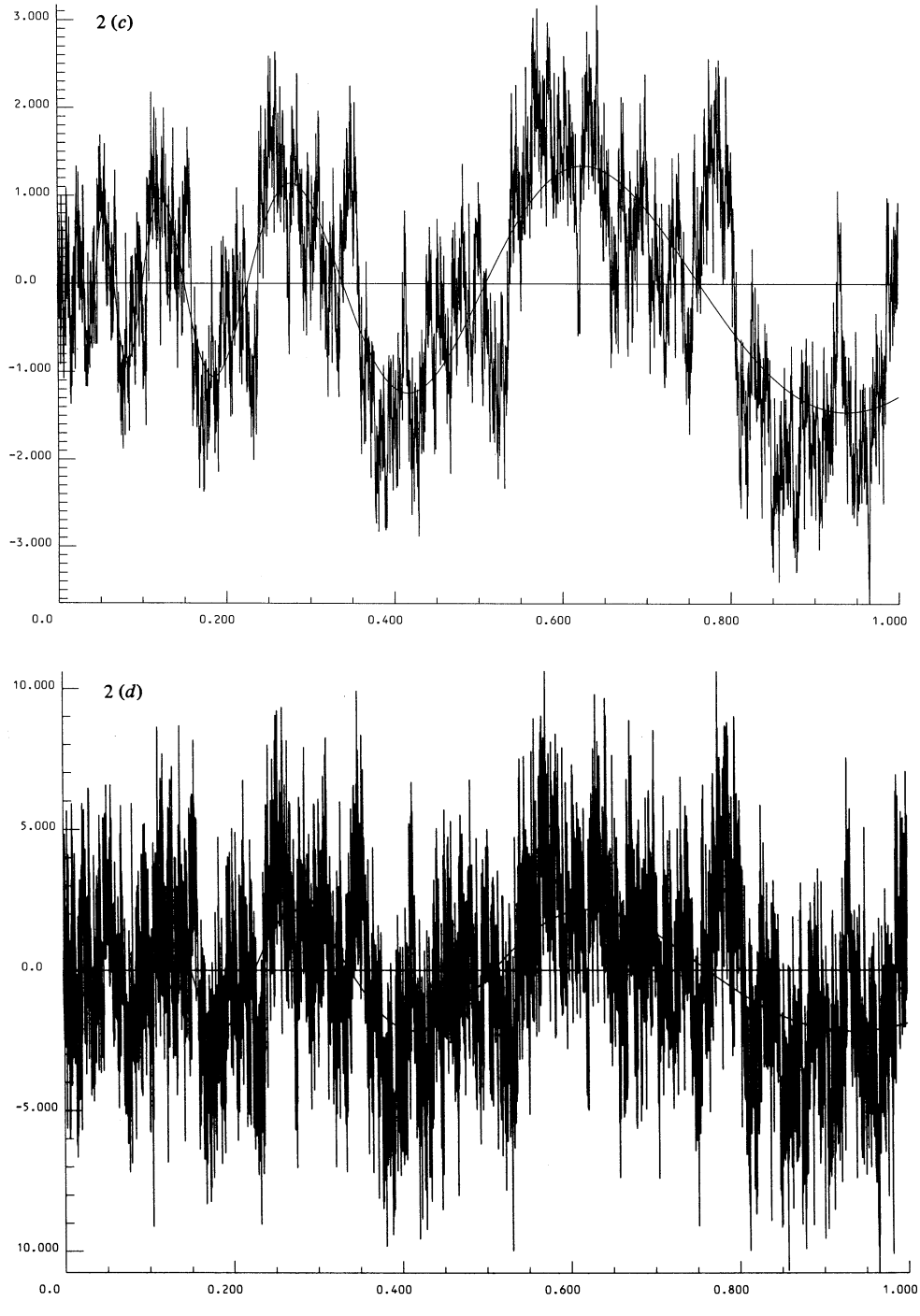

FIGURE 2. Weierstrass–Mandelbrot alternating-sign sine fractal function $A(t)$, range $0 \leqslant t \leqslant 1$, $\gamma = 1.5$: (*a*) $D = 1.2$; (*b*) $D = 1.5$; (*c*) $D = 1.8$; (*d*) $D = 1.99$.

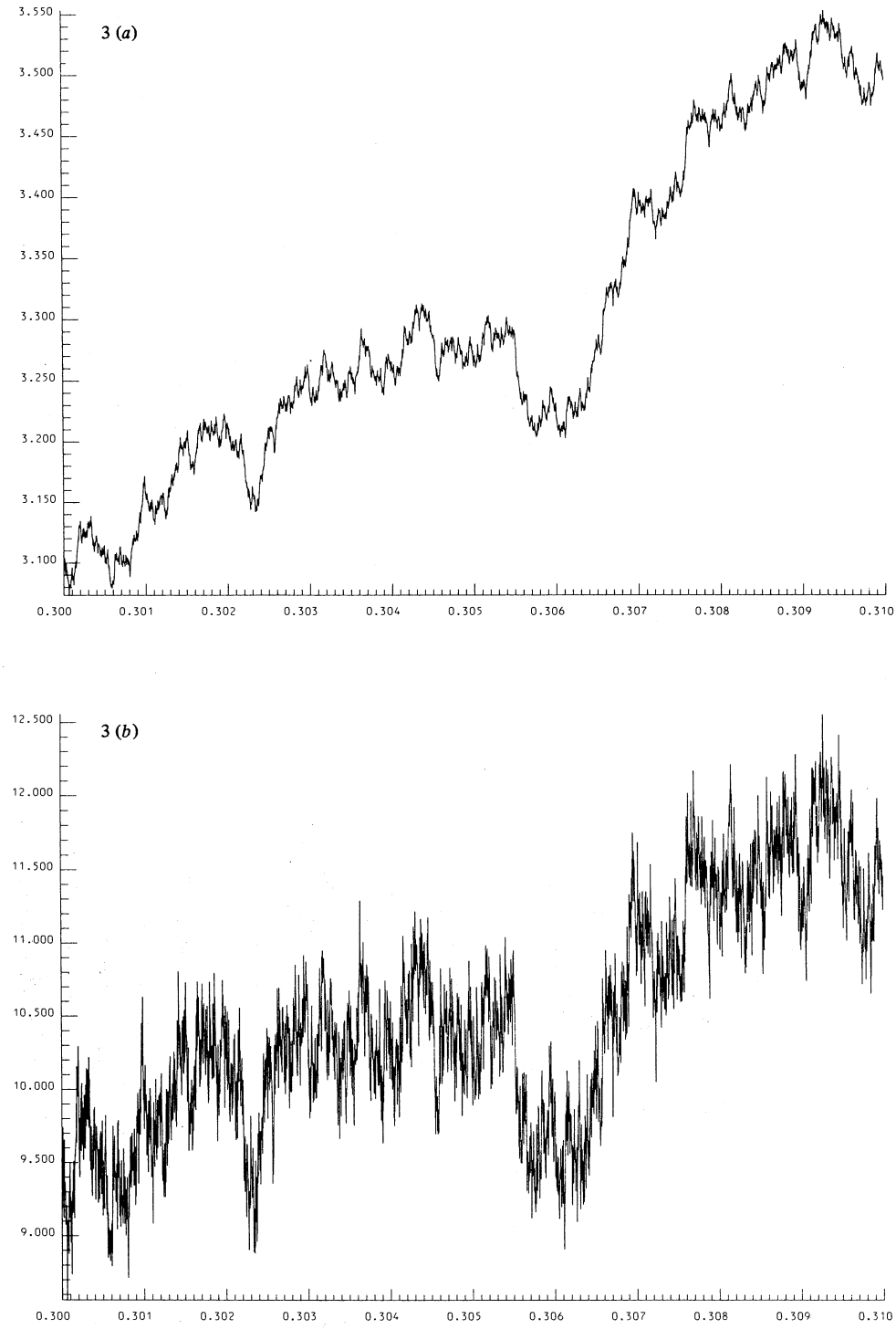

FIGURE 3 (*a*), (*b*) For legend see page 469.

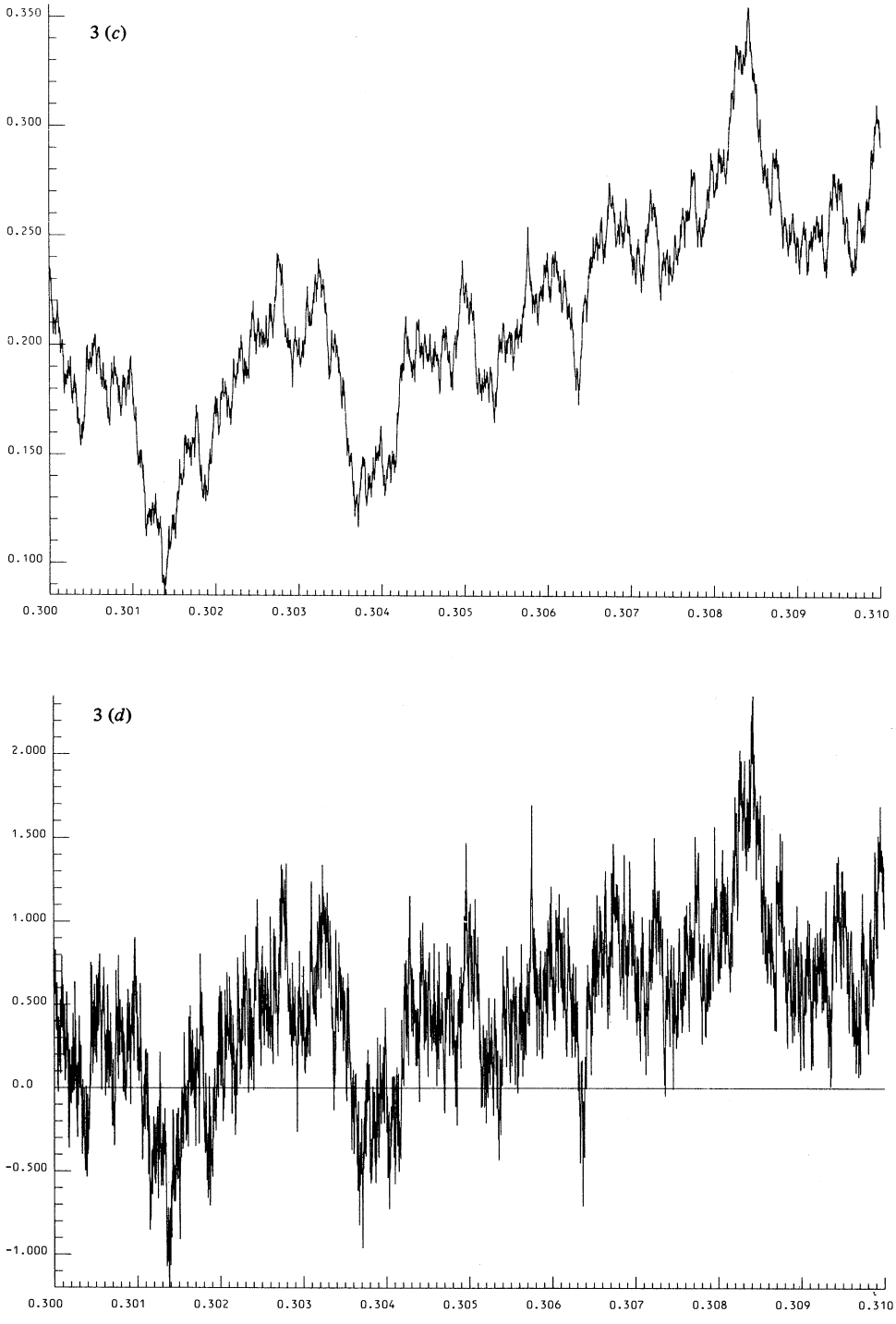

FIGURE 3. Weierstrass–Mandelbrot fractal function on range $0{\cdot}30 \leqslant t \leqslant 0.31, \gamma = 1.5$: (*a*) $C(t)$ with $D = 1.5$; (*b*) $C(t)$ with $D = 1.8$; (*c*) $A(t)$ with $D = 1.5$; (*d*) $A(t)$ with $D = 1.8$.

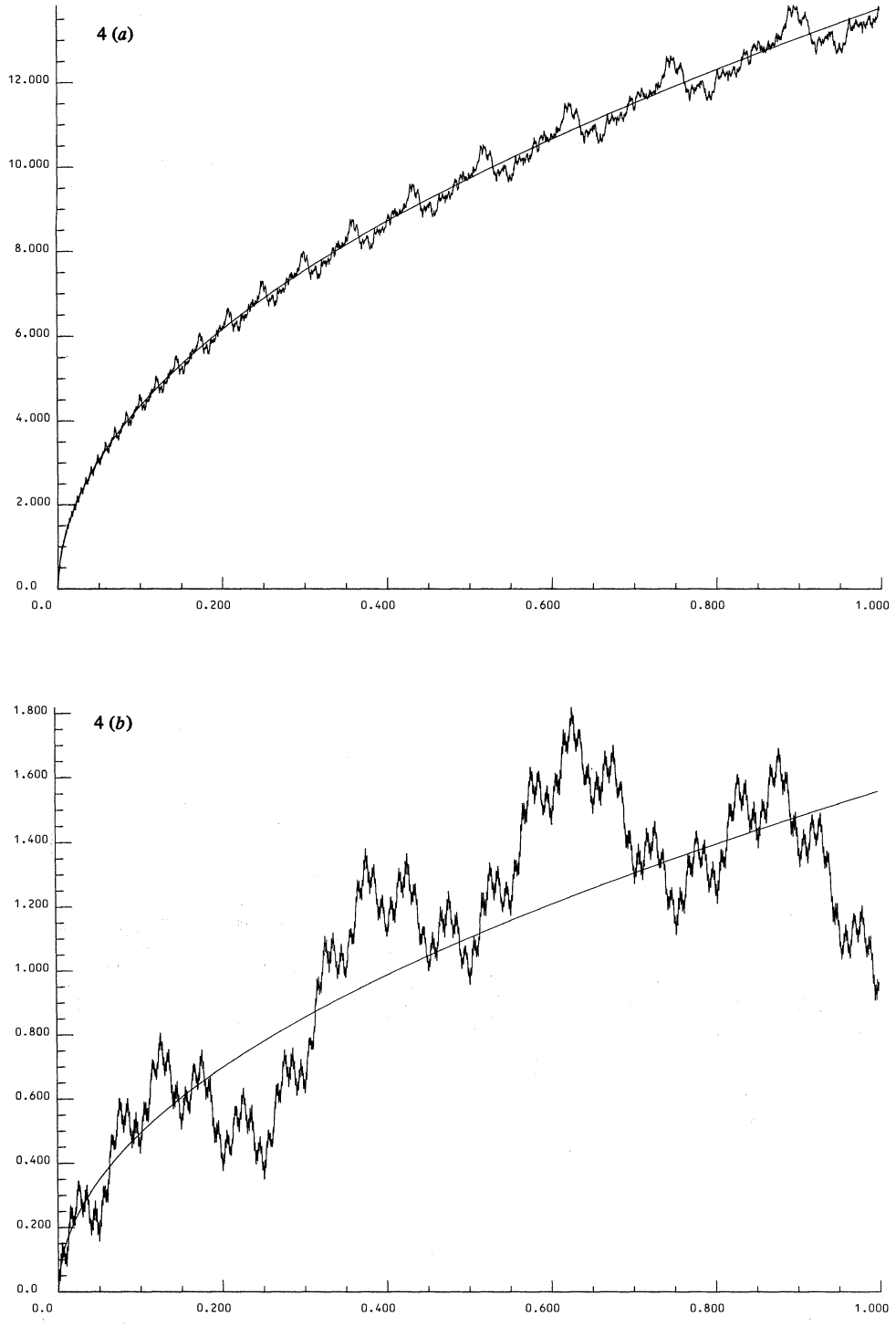

FIGURE 4 (*a*), (*b*) For legend see page 471.

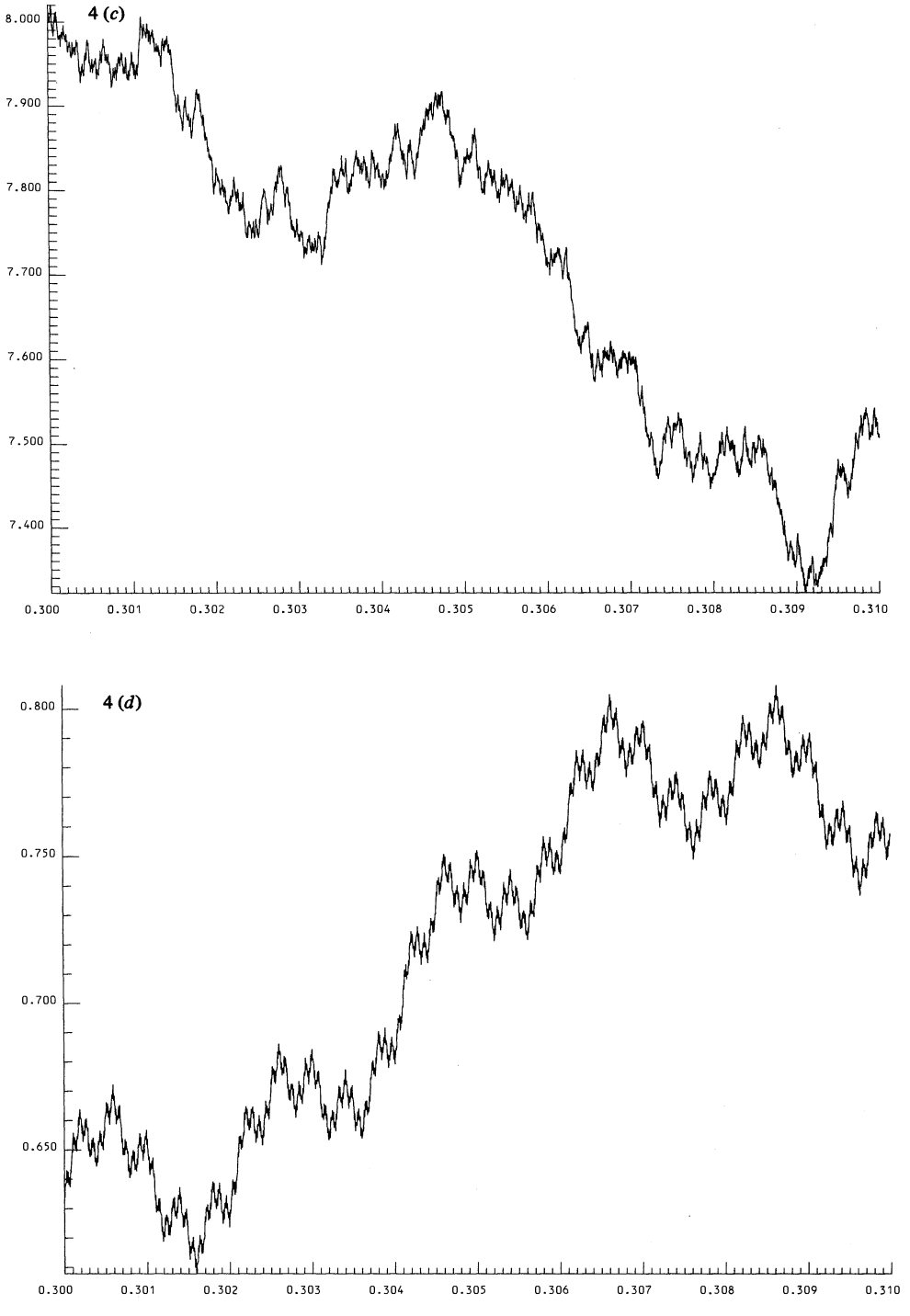

FIGURE 4. Weierstrass–Mandelbrot cosine fractal function $C(t)$, $D = 1.5$: (*a*) $0 \leqslant t \leqslant 1$, $\gamma = 1.2$; (*b*) $0 \leqslant t \leqslant 1$, $\gamma = 5$; (*c*) $0.30 \leqslant t \leqslant 0.31$, $\gamma = 1.2$; (*d*) $0.30 \leqslant t \leqslant 0.31$, $\gamma = 5$.

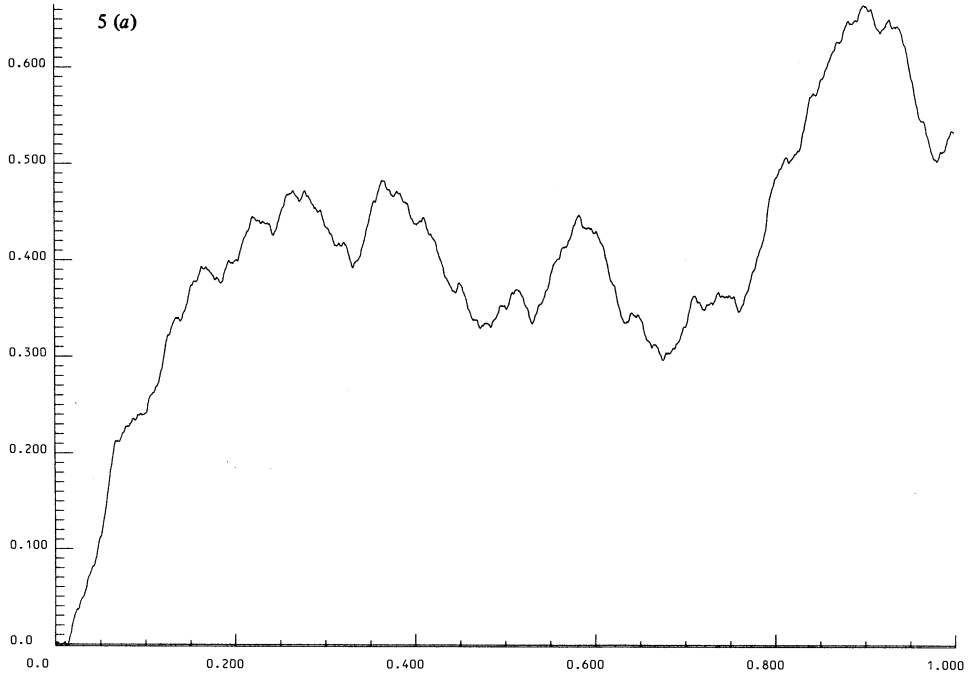

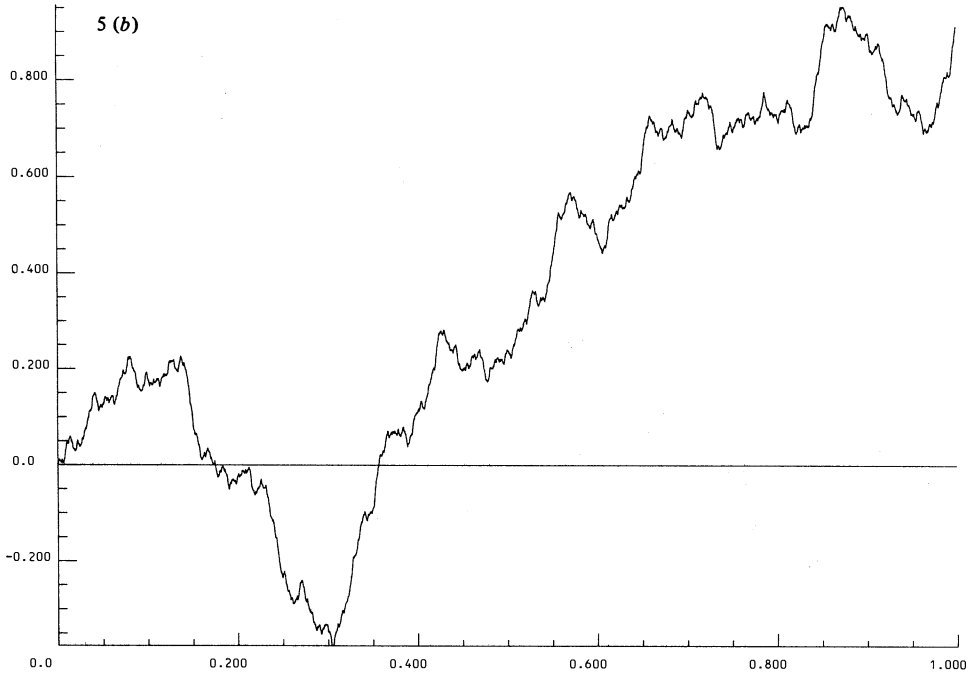

FIGURE 5 (*a*), (*b*) For legend see page 474.

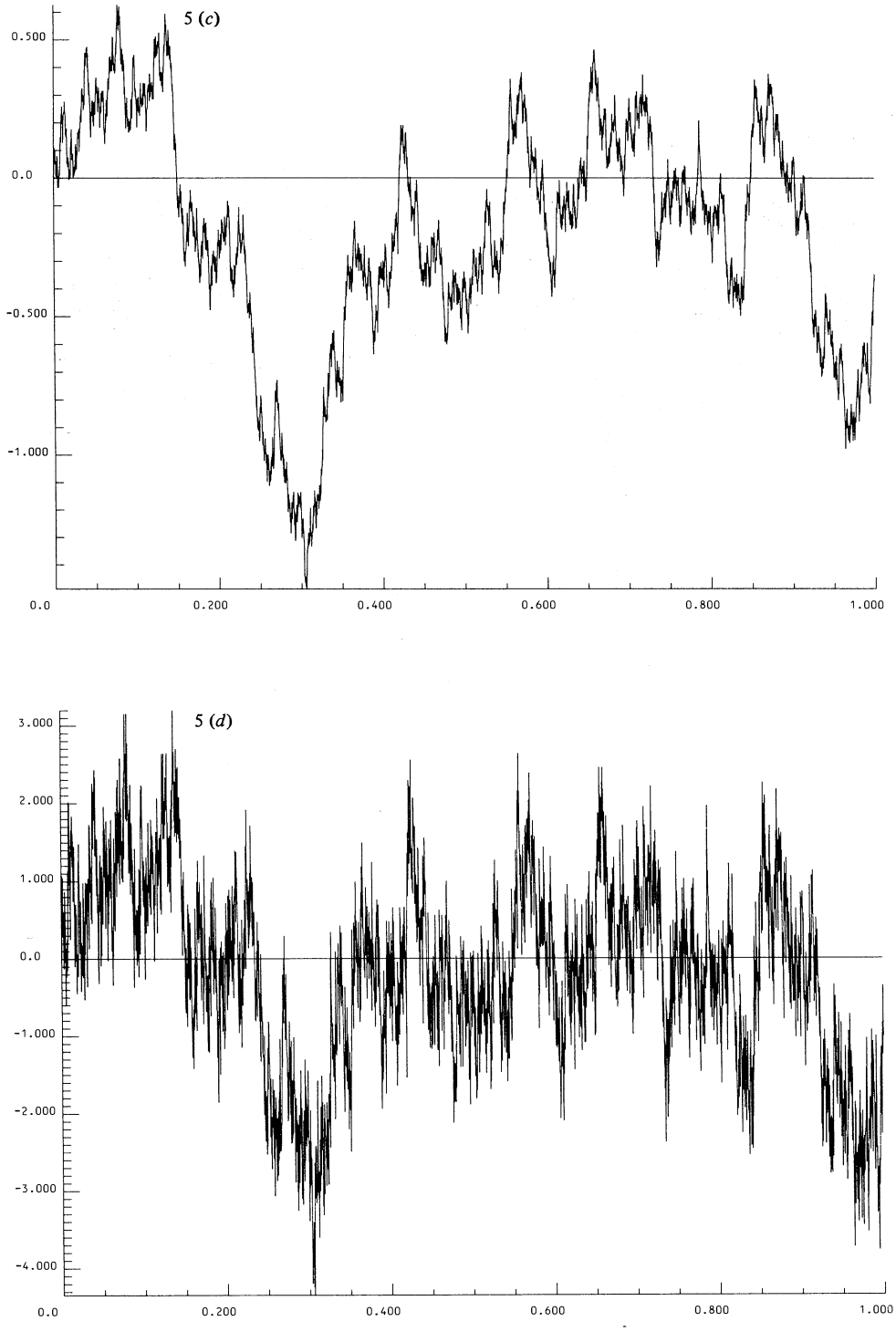

FIGURE 5 (*c*), (*d*) For legend see page 474.

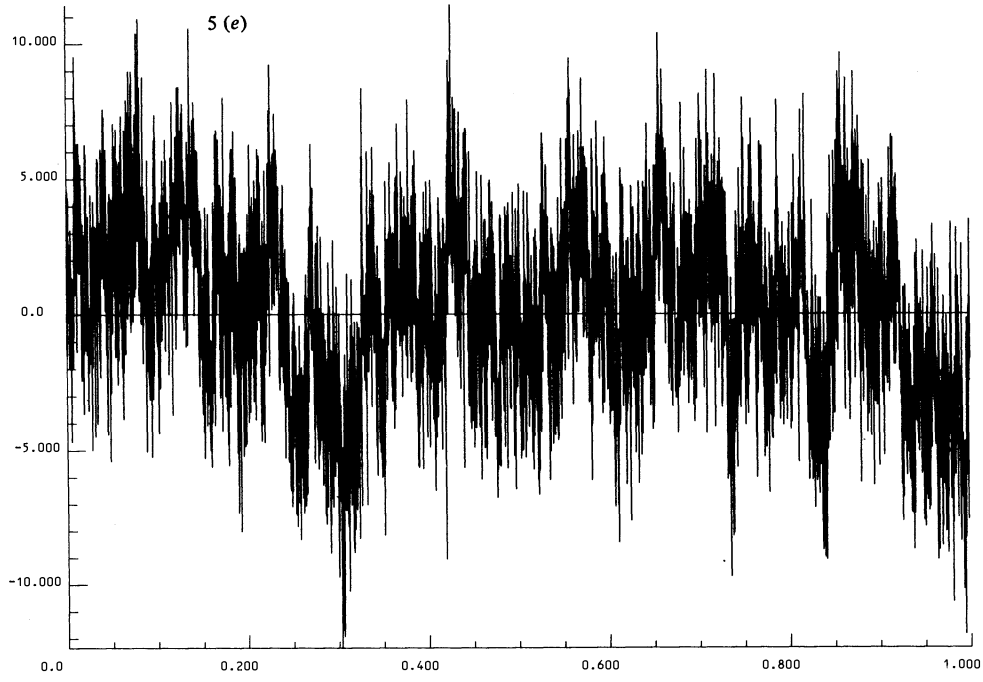

FIGURE 5. Weierstrass–Mandelbrot random fractal function, range $0 \leqslant t \leqslant 1$, $\gamma = 1.5$: (*a*) $D = 1$; (*b*) $D = 1.2$; (*c*) $D = 1.5$; (*d*) $D = 1.8$; (*e*) $D = 1.99$.

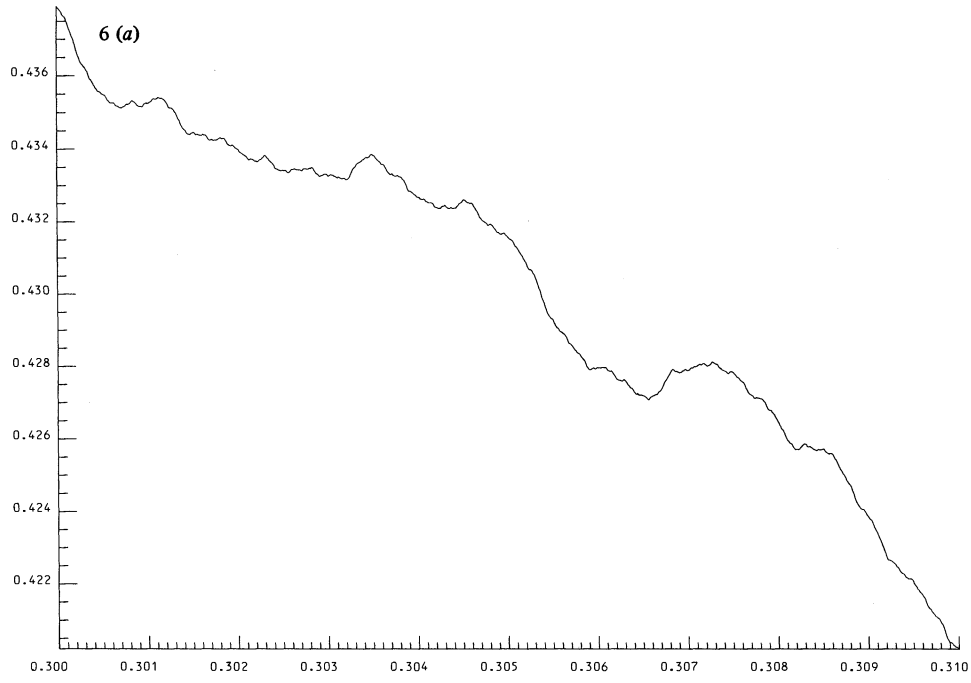

FIGURE 6 (*a*) For legend see page 476.

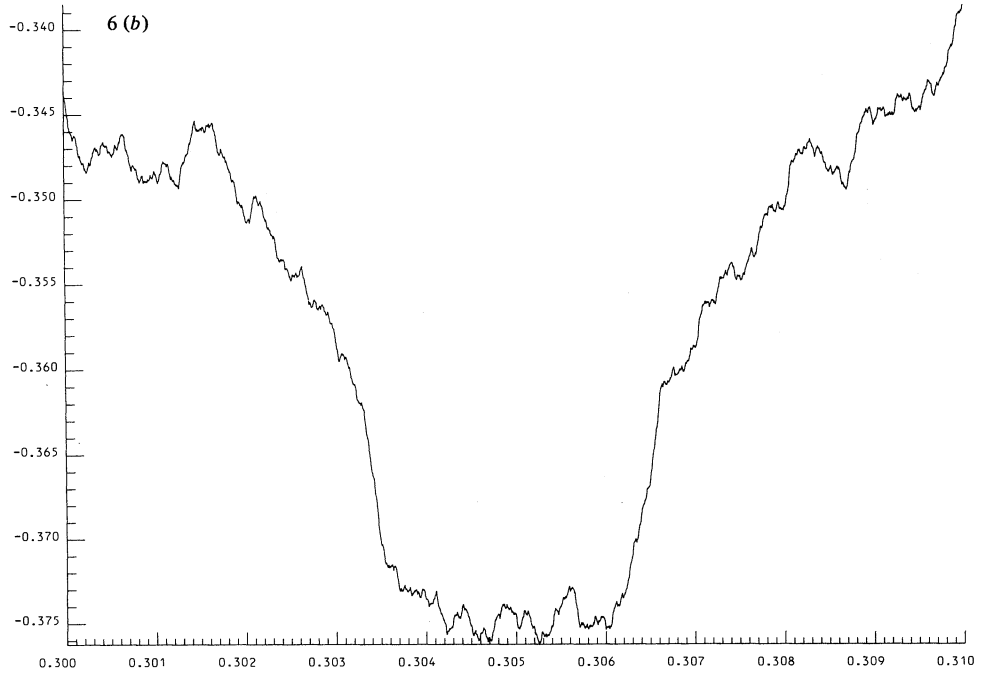

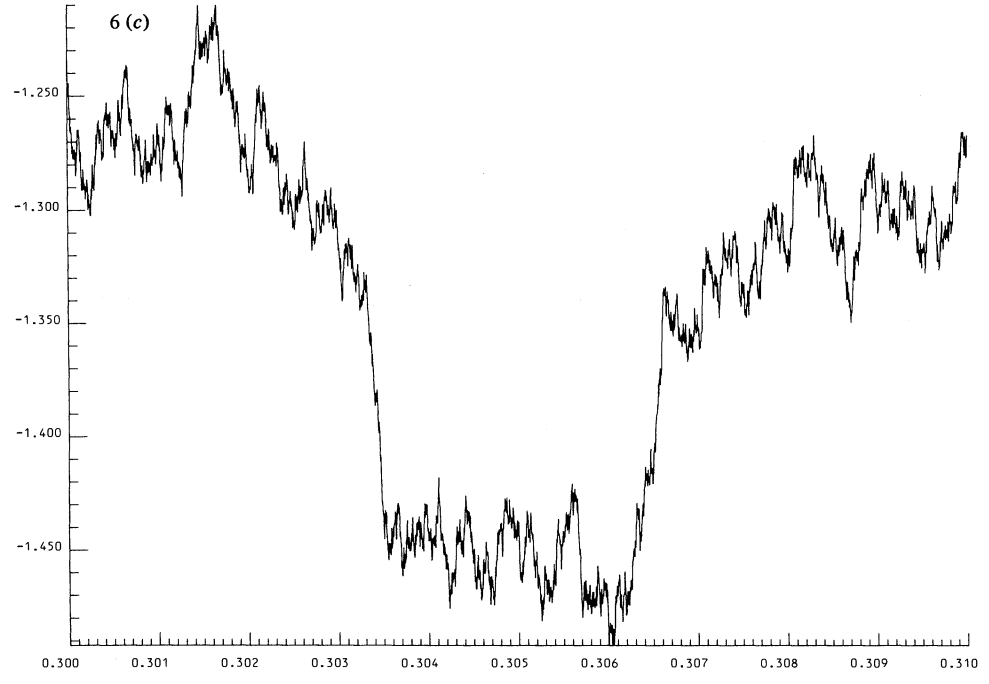

FIGURE 6 (*b*), (*c*) For legend see page 476.

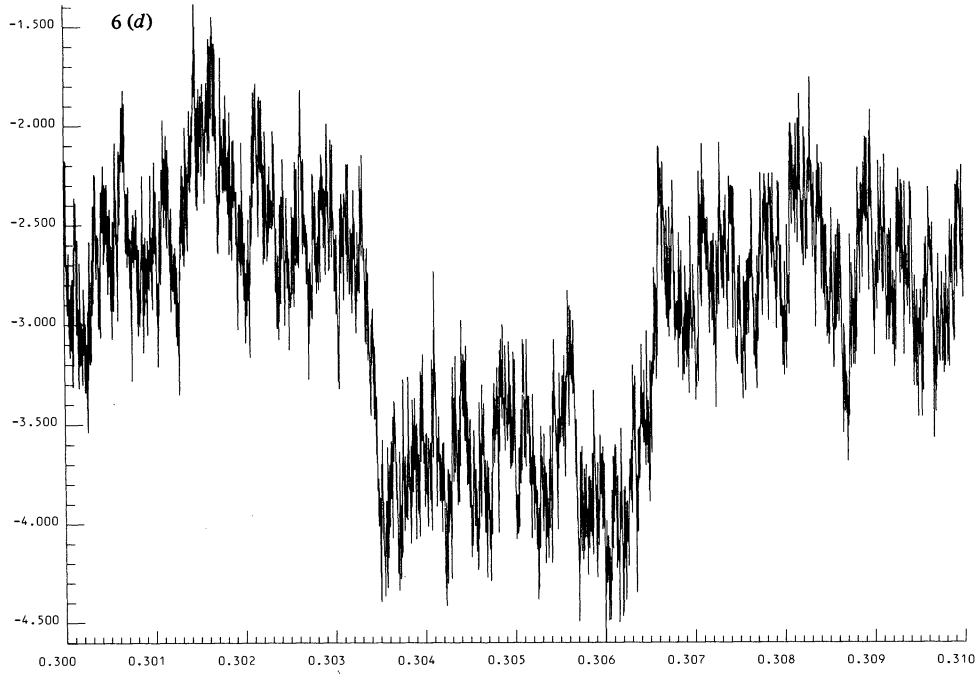

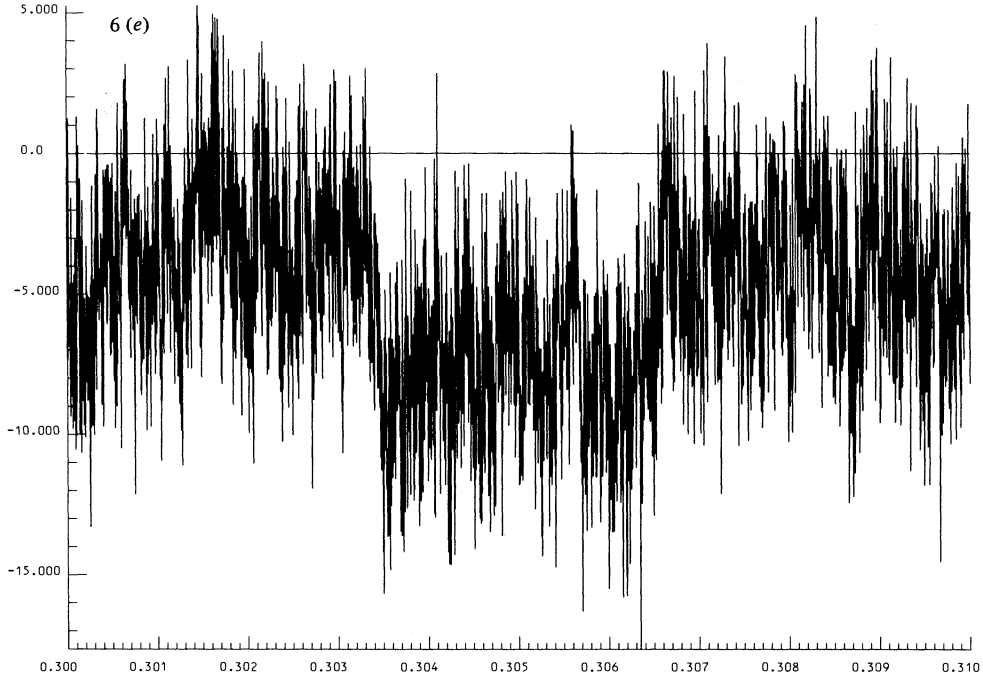

FIGURE 6. As figure 5 but with range $0.30 \leqslant t \leqslant 0.31$.

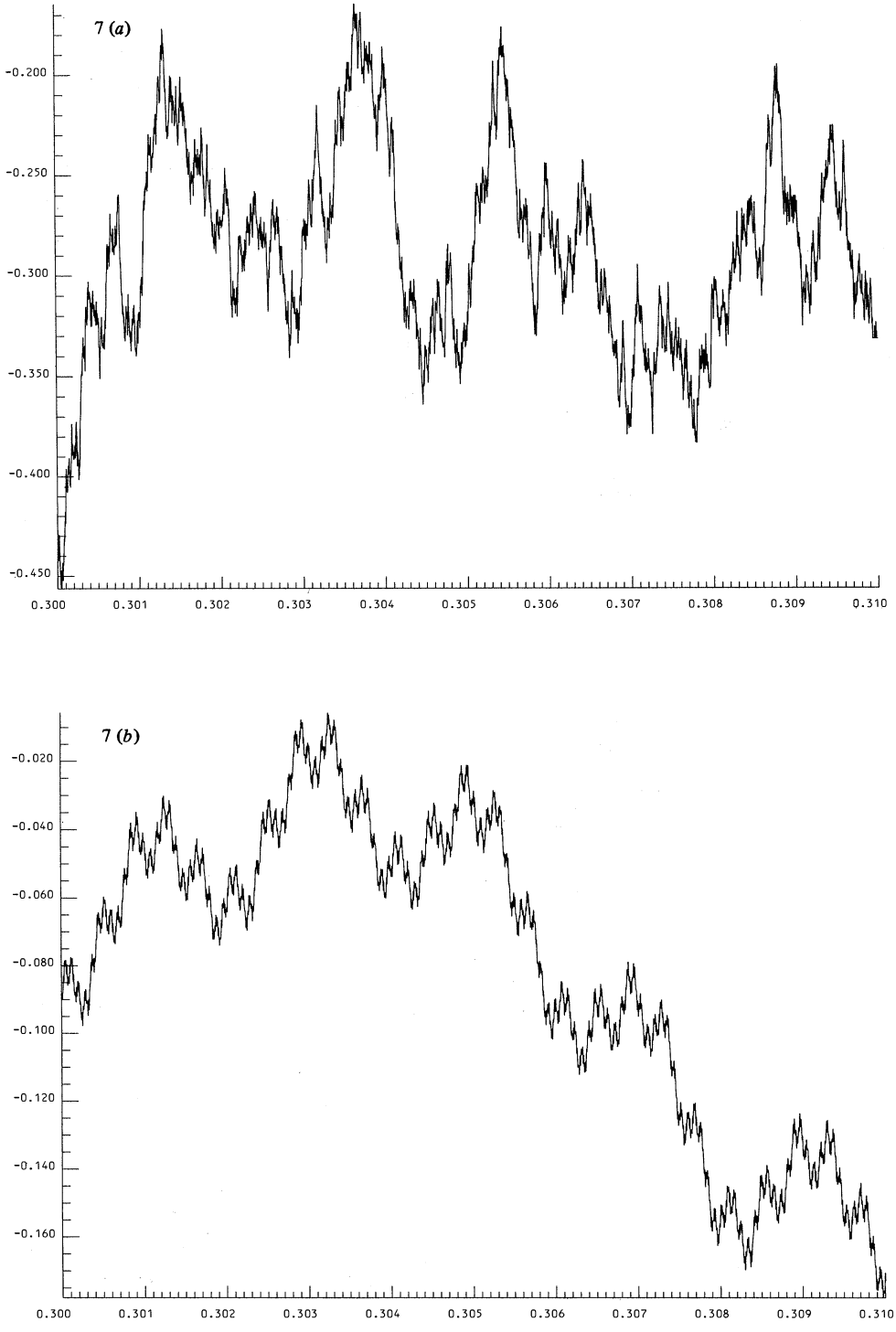

FIGURE 7 (*a*), (*b*) For legend see page 478.

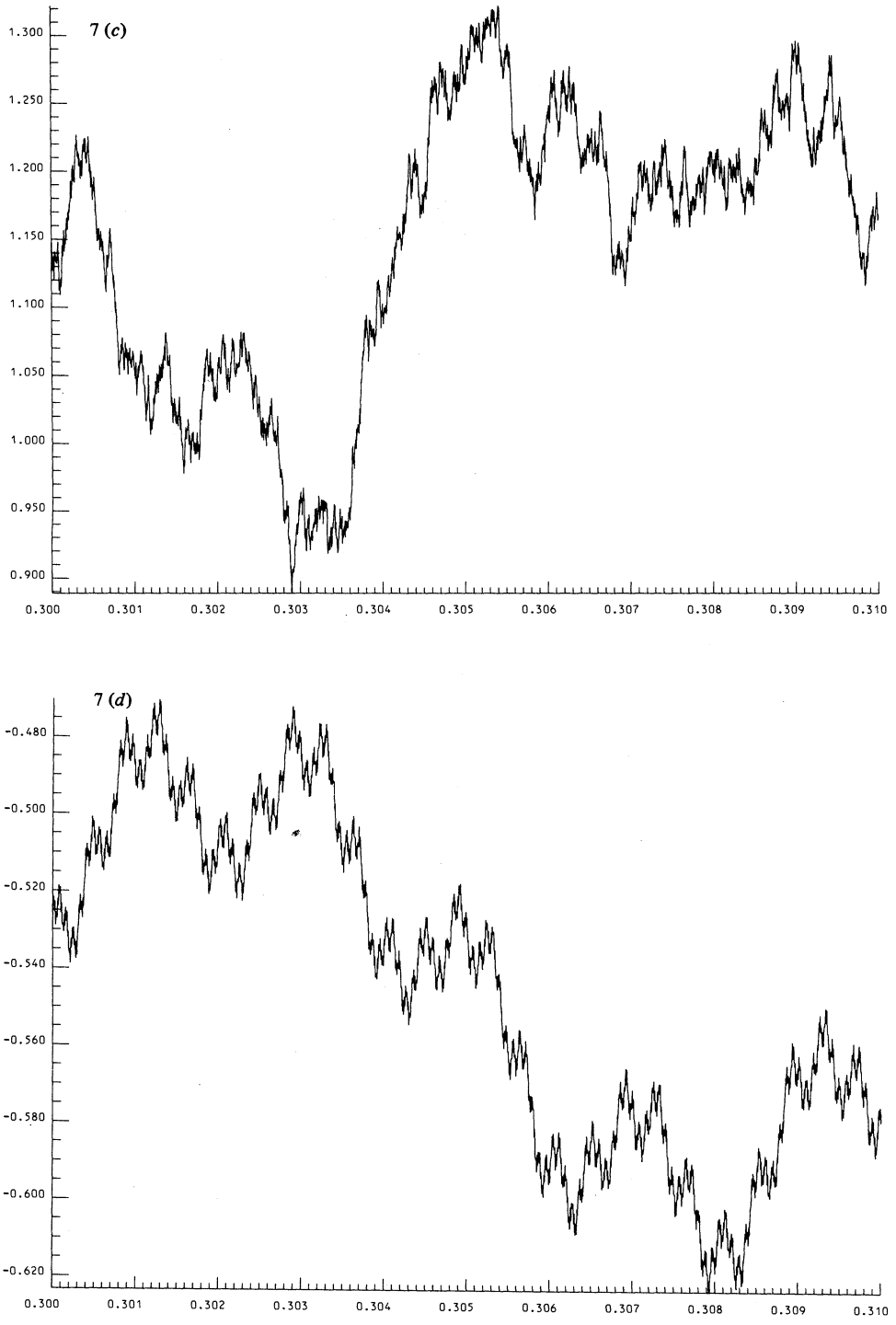

FIGURE 7. Weierstrass–Mandelbrot fractal function, range $0.30 \leqslant t \leqslant 0.31$, $D = 1.5$: (*a*) $A(t)$, $\gamma = 1.2$; (*b*) $A(t)$, $\gamma = 5$; (*c*) random, $\gamma = 1.2$; (*d*) random, $\gamma = 5$.

To understand the statistics of W, we introduce ensemble averages, denoted by $\langle\,\rangle_e$ and defined as mean values over all possible sets $\{\phi_n\}$. Next we calculate the variance $V(\tau)$ of the increments of W, namely

$$V(\tau) \equiv \langle |W(t+\tau)-W(t)|^2\rangle_e$$

$$= \prod_{n=-\infty}^{\infty} \int_0^{2\pi} \frac{d\phi_n}{2\pi} \sum_{l=-\infty}^{\infty} \sum_{m=-\infty}^{\infty} \frac{(e^{i\gamma^l t}-e^{i\gamma^l(t+\tau)})(e^{-i\gamma^m t}-e^{-i\gamma^m(t+\tau)})e^{i(\phi_l-\phi_m)}}{\gamma^{(2-D)(l+m)}}$$

$$= 2\sum_{n=-\infty}^{\infty} \frac{(1-\cos\gamma^n\tau)}{\gamma^{(4-2D)n}}. \tag{12}$$

This is independent of t, and, together with the easily-proved result $\langle (W(t+\tau)-W(t))\rangle_e = 0$, implies that the randomness of the increments of W is stationary. W itself is not a stationary random function, since its variance, as obtained from (12) and $W(0) = 0$, is

$$\langle |W(t)|^2\rangle_e = V(t), \tag{13}$$

which does depend on t.

$V(\tau)$ is a measure of the correlation between the values of W at points separated by τ, and the formula (12) holds not only for the ensemble average at fixed t but also for the t-average for a given function in the ensemble, i.e.

$$\langle |W(t+\tau)-W(t)|^2\rangle_t \equiv \lim_{T\to\infty} \frac{1}{2T}\int_{-T}^{T} dt\,|W(t+\tau)-W(t)|^2 = V(\tau). \tag{14}$$

Comparison of (12) with the cosine series (4) shows that $V(\tau)$ represents a strange correlation, which itself has the form of a Weierstrass function with $4-2D$ replacing $2-D$. Thus $V(\tau)$ is a fractal function, with dimension $2(D-1)$ if $D > 1.5$, but is a differentiable function if $D < 1.5$. For all D, $V(\tau)$ obeys the scaling law

$$V(\gamma\tau) = \gamma^{4-2D}\,V(\tau) \tag{15}$$

By analogy with (9), the trend of V is

$$V(\tau) \approx \frac{\tau^{4-2D}\,\Gamma(2D-2)\cos\pi D}{\ln\gamma\,(2-D)\,(2D-3)}, \tag{16}$$

which is an exact representation of (12) as $\gamma \to 1$.

The power spectrum $S(\omega)$ of W is proportional to the square of its Fourier transform, or to the Fourier transform of the time-average correlation $\langle W(t+\tau)W^*(t)\rangle_t$, and is given, apart from a zero-frequency term, by

$$S(\omega) = \sum_{n=-\infty}^{\infty} \frac{\delta(\omega-\gamma^n)}{\gamma^{(4-2D)n}}. \tag{17}$$

To approximate this discrete Weierstrass spectrum by a continuous spectrum $\bar{S}(\omega)$, we average $S(\omega)$ over a range $\Delta\omega$ including Δn frequencies γ^n, so that

$$\bar{S}(\omega) \equiv \frac{1}{\Delta\omega}\int_{-\frac{1}{2}\Delta w}^{\frac{1}{2}\Delta w} \mathrm{d}\omega' S(\omega+\omega') \approx \frac{\Delta n}{\Delta\omega\gamma^{(4-2D)\,n(\omega)}}, \tag{18}$$

where $n(\omega) = \ln\omega/\ln\gamma$. This gives

$$\bar{S}(\omega) \approx \frac{\mathrm{d}n(\omega)/\mathrm{d}\omega}{\gamma^{(4-2D)\,n(\omega)}} = \frac{1}{\ln\gamma\,\omega^{5-2D}}. \tag{19}$$

In the limit $\gamma \to 1$ this is an exact result, and the Gaussian random fractal function $W(t)$ then has a continuous spectrum.

4. Fractal dimension of the graph of W

Following Orey (1970), we use the 'potential' definition of fractal dimension D (Mandelbrot 1977). Let positive charge uniformly cover the t axis with unit density. Move this charge up or down until it hits the graph of Re $W(t)$. Now write the electrostatic energy (per unit length of the t axis) of this fractal line of charge, by employing a modified Coulomb law where the interaction potential of two unit charges separated by r is r^{-d} where d need not be unity. This energy is $E(d)$, where

$$E(d) = \tfrac{1}{2}\lim_{T\to\infty}\frac{1}{2T}\int_{-T}^{T}\mathrm{d}t\int_{-T}^{T}\mathrm{d}t'\,[(\mathrm{Re}\,W(t)-\mathrm{Re}\,W(t'))^2+(t-t')^2]^{-\frac{1}{2}d}. \tag{20}$$

Then the fractal dimension is defined as the greatest d for which $E(d)$ is not infinite.

To study the convergence of this double integral, define $\tau \equiv t'-t$ and

$$\Delta(\tau, t) \equiv \mathrm{Re}\,(W(t+\tau)-W(t)), \tag{21}$$

so that

$$E(d) = \tfrac{1}{2}\lim_{T\to\infty}\frac{1}{2T}\int_{-T}^{T}\mathrm{d}t\int_{-T-t}^{T-t}\mathrm{d}\tau\,[\Delta^2(\tau,t)+\tau^2]^{-\frac{1}{2}d}. \tag{22}$$

The next step, whose legitimacy will be discussed presently, is to replace E by its ensemble average $\langle E\rangle_{\mathrm{e}}$. This gives

$$E(d) = \tfrac{1}{2}\lim_{T\to\infty}\frac{1}{2T}\int_{-T}^{T}\mathrm{d}t\int_{-T-t}^{T-t}\mathrm{d}\tau\int_{-\infty}^{\infty}\mathrm{d}\Delta\,\frac{P(\Delta,\tau)}{(\Delta^2+\tau^2)^{\frac{1}{2}d}}, \tag{23}$$

where $P(\Delta,\tau)$ is the probability that the increment in Re W between t and $t+\tau$ will be Δ, and is independent of t because of the statistical stationarity of the increments. P is a Gaussian function of Δ, whose variance $\langle\Delta^2\rangle_{\mathrm{e}}$ is $\frac{1}{2}V(\tau)$ (equation 12):

$$P(\Delta,\tau) = \mathrm{e}^{-\Delta^2/V(\tau)}/\sqrt{(\pi V(\tau))}. \tag{24}$$

Therefore (23) becomes

$$E(d) = \frac{1}{2}\int_{-\infty}^{\infty}\mathrm{d}\Delta\int_{-\infty}^{\infty}\mathrm{d}\tau\,\frac{\mathrm{e}^{-\Delta^2/V(\tau)}}{\sqrt{(\pi V(\tau))}\,(\Delta^2+\tau^2)^{\frac{1}{2}d}}. \tag{25}$$

We obtained this formula by replacing the t-average (22), over a *given* function W, by the ensemble average (23), over *all* functions W at fixed t. Is this justified? Let the series (1) be truncated to include N terms, where later we shall take the

limit $N \to \infty$. The N phases ϕ_n can be considered as angle coordinates on an N-dimensional torus, each point of which represents a function W in the ensemble. Ensemble-averaging corresponds to fixing t and integrating over the torus. Now, t-averaging, i.e. fixing $\{\phi_n\}$ and integrating over t, has the same effect as fixing t and integrating along a curve on the torus whose equation is given parametrically by

$$\phi_n = \text{constant} + \gamma^n t' \quad (-\infty < t' < +\infty), \tag{26}$$

as is clear by inspection of (1). This curve winds round the torus with angular frequencies γ^n. The resulting t-average is equal to an ensemble average, provided the curve eventually covers the torus uniformly. But by an ergodic theorem for tori (Arnol'd 1978) this will happen provided the frequency ratios are irrational, i.e. *if γ is irrational.* This result is independent of N and so holds as $N \to \infty$.

Thus (25) is correct for almost all functions W, even those which are deterministic, the only possible exceptions being the set of measure zero with rational γ. What about these exceptions? Equation (1) shows that W, considered as a function of γ, is continuous (although it may not be differentiable). This strongly suggests that the fractal dimension is a continuous function of γ, and so its value at rational γ equals its value at any neighbouring irrational γ. 'Experimental' support for this argument was provided by a calculation of (1) with γ equal to the highly irrational number $(\sqrt{5}+1)/2 = 1.618\ldots$, $D = 1.5$ and random phases; the resulting graph closely resembled figure 5*c*, for which γ has the low-order rational value 1.5. We conclude that the fractal dimension of every member in the ensemble of functions W is determined by the convergence of (25).

Now we argue that the fractal dimension as given by (25) is actually independent of γ. What is important is the behaviour of the integrand near the origin $\Delta = \tau = 0$. This depends on $V(\tau)$, which by (12) and (15) is a very complicated function near $\tau = 0$. Since V is never negative, it is plausible that the convergence of (25) is determined by the trend (16) of V , i.e. by its average over ranges τ to $\gamma\tau$, which are infinitesimal when $\tau \approx 0$. Assuming this, and ignoring irrelevant constants, we obtain

$$E(d) \propto \int_{-\infty}^{\infty} \mathrm{d}\Delta \int_{-\infty}^{\infty} \mathrm{d}\tau \frac{\exp\{-\Delta^2/|\tau|^{4-2D}\}}{|\tau|^{2-D}(\Delta^2+\tau^2)^{\frac{1}{2}d}}, \tag{27}$$

which is indeed independent of γ. In the limit $\gamma \to 1$, (27) is an exact representation of (25).

The final step is to transform to polar coordinates r, θ in the Δ, τ plane, giving

$$E(d) \propto \int_0^{2\pi} \mathrm{d}\theta \int_0^{\infty} \mathrm{d}r \frac{r^{D-1-d} \exp\{-r^{2(D-1)} \cos^2\theta/(\sin\theta)^{4-2D}\}}{(\sin\theta)^{2-D}} \tag{28}$$

As $r \to 0$ the exponential factor is unity except in a narrow sector of angular width $\theta \sim r^{(D-1)/(2-D)}$. The singularity $(\sin\theta)^{-(2-D)}$ is integrable, so convergence is governed by the factor r^{D-1-d}, and requires

$$d < D. \tag{29}$$

Therefore the fractal dimension of the graph of W is D in all cases, as we have assumed throughout this paper.

Of course these arguments are far from rigorous, and the possibility remains that W has a fractal dimension differing from D by a quantity that vanishes as $\gamma \to 1$. 'Experimental' evidence suggests otherwise: the functions $C(t)$ $(0.30 \leqslant t \leqslant 0.31)$ for $D = 1.5$, shown on figures 3*a*, 4*c* and 4*d* for $\gamma = 1.5$, 1.2 and 5, all display approximately the same degree of irregularity; so do the corresponding graphs of $A(t)$ (figures 3*c*, 7*a*, *b*), and the random fractals (figures 6*c*, 7*c*, *d*). Moreover, the fact that the three groups of functions, $C(t)$, $A(t)$ and random, all resemble one another supports our earlier conclusion that the fractal dimension is the same for all sets of phases $\{\phi_n\}$.

5. Quantum potential with a Weierstrass spectrum

A striking feature of W is its Weierstrass spectrum γ^n, and it is natural to ask whether any operator possesses such a spectrum (excluding such trivial possibilities as the eigenvalues of $\exp[(\hat{l}_z/\hbar)\ln\gamma]$, where $\hat{l}_z$ is the angular momentum operator). We seek a potential well $U(x)$ of such a form that the discrete energy levels for a non-relativistic particle are

$$E_n = -\mathscr{E}_0\gamma^{-n} \quad (-\infty < n < \infty). \tag{30}$$

These levels are defined by eigenfunctions $\psi_n(x)$ on the positive x axis, and satisfy the Schrödinger equation

$$\frac{\mathrm{d}^2\psi_n(x)}{\mathrm{d}x^2} + [E_n - U(x)]\psi_n(x) = 0 \quad (\psi_n(0) = \psi_n(\infty) = 0). \tag{31}$$

The spectrum (30) has an infinitely deep ground state ($n = -\infty$) and excited states clustering to a limit point at $E = 0$ ($n = +\infty$). Now, any 'regular' potential, i.e. one that is bounded from below or diverges as $x \to 0$ more slowly than $-1/4x^2$, has a ground state at finite energy. On the other hand, any so-called 'singular' potential (Frank, Land & Spector 1971), which diverges faster than $-1/4x^2$, has wave functions oscillating infinitely rapidly as $x \to 0$ and so would appear to possess a continuous spectrum of bound states. It therefore seems that the Weierstrass spectrum, being both bottomless and discrete, can only be generated by a potential that in some sense is neither regular nor singular.

Consider, however, the weakly singular potential

$$U(x) = -A/x^2, \tag{32}$$

where $A > \frac{1}{4}$. The solution of (31) which decays at infinity is, for any negative energy E,

$$\psi(x) = \mathrm{B}\sqrt{x}\,K_{i\sqrt{(A-\frac{1}{4})}}(x\sqrt{(-E)}), \tag{33}$$

where K_ν denotes the modified Bessel function of the second kind with order ν

(Abramowitz & Stegun 1964), and B is a normalization constant. As $x \to 0$, standard formulae give

$$\psi(x) \to \frac{B\pi\sqrt{x}}{\sinh \pi\sqrt{(A-\frac{1}{4})}\,|\Gamma(1+\mathrm{i}\sqrt{(A-\frac{1}{4})})|} \times \sin\{\sqrt{(A-\tfrac{1}{4})}\ln(\tfrac{1}{2}x\sqrt{-E}) - \arg\Gamma(1+\mathrm{i}\sqrt{(A-\tfrac{1}{4})})\}. \quad (34)$$

This tends to zero, suggesting that a bound state exists for any negative E, i.e. that the spectrum is continuous. (If $A < \frac{1}{4}$, solutions of the form (33) diverge at the origin and there are no bound states.)

Now, as Frank *et al.* (1971) point out, discreteness can be imposed by demanding that any two solutions (33) with energies E_1 and E_2 are orthogonal. Using the result

$$\int_{-\infty}^{\infty} \mathrm{d}z\, z\, K_\nu(az)\, K_\nu(bz) = \frac{\pi(ab)^{-\nu}(a^{2\nu}-b^{2\nu})}{2\sin\nu\pi(a^2-b^2)} \quad (35)$$

(Gradshteyn & Ryzhik 1965), we find that orthogonality implies

$$\exp\{\mathrm{i}\sqrt{(A-\tfrac{1}{4})}\ln(-E_1)\} = \exp\{\mathrm{i}\sqrt{(A-\tfrac{1}{4})}\ln(-E_2)\}, \quad (36)$$

so

$$E_1/E_2 = \exp\{2\pi n/\sqrt{(A-\tfrac{1}{4})}\}, \quad (37)$$

where n is an integer. Therefore the levels do indeed form a geometric progression, and the spectrum can be brought into the Weierstrass form (30) if one level is fixed at $-\mathscr{E}_0$ and A is chosen to be

$$A = \tfrac{1}{4} + 4\pi^2/\ln^2\gamma. \quad (38)$$

The same result can be obtained from the exact eigenstates of the potential

$$U(x) = -A/(x+\delta)^2 \quad (39)$$

as $\delta \to 0$.

It is possible that the attractive inverse-square potential might be the only one with a Weierstrass spectrum, but we are unable to prove this. There may well be other vibrating systems with a Weierstrass spectrum (e.g. variable-density strings), but we do not know any.

Appendix: Computational procedure

The Weierstrass–Mandelbrot function W was computed directly from the series (1), using complex double-precision arithmetic and Re W or Im W plotted against t. The summation over n was truncated at $n_{\min}(<0)$ and $n_{\max}(>0)$. $n_{\min}$ was chosen so that the sum of the neglected terms $-\infty < n < n_{\min}$ could not be perceived by eye at the scales plotted. A similar criterion was not used for $n_{\max}$, because it sometimes (i.e. for $\gamma \to 1$ and $D \to 2$) resulted in such large arguments $\gamma^n t$ that the trigonometric functions in (1) could not be computed. This difficulty is a direct consequence of W having a Weierstrass spectrum, which makes the frequencies γ^n

increase very rapidly with n. Therefore $n_{\max}$ was chosen so that the neglected terms $n > n_{\max}$ corresponded to oscillatory contributions to W whose t-wavelengths could not be perceived by eye at the scales plotted. This new criterion resulted in much smaller values for $n_{\max}$. In those cases where it was possible to compare the results obtained using both criteria, there was no visible difference, except for one case, namely the function $C(t)$. Here there were non-oscillatory terms, whose sum for $n > n_{\max}$ caused an overall shift in the function when the smaller $n_{\max}$ was used; therefore these terms were summed analytically and added to the computed function.

References

Abramowitz, M. & Stegun, I. A. 1964 *Handbook of mathematical functions*. Washington: U.S. National Bureau of Standards.

Arnol'd, V. I. 1978 *Mathematical methods to classical mechanics*. New York: Springer, §51.

Frank, W. M., Land, D. J. & Spector, R. M. 1971 *Rev. Mod. Phys.* **43**, 36–98.

Gradshteyn, I. S. & Ryzhik, I. M. 1965 *Table of integrals, series and products*. New York: Academic Press. p. 672.

Lighthill, M. J. 1958 *Introduction to Fourier analysis and generalized functions*, p. 67. Cambridge University Press.

Mandelbrot, B. B. 1977 *Fractals: form, chance and dimension*. San Francisco: Freeman.

Nye, J. F. 1970 *Proc. R. Soc. Lond.* A **315**, 381–403.

Orey, S. 1970 *Z. Wahrscheinlichkeitstheor.* **15**, 249–256.

Press, W. H. 1978 *Comments Astrophys.* **7**, 103–119.

Rice, S. O. 1944 *Bell. Tech. J.* **23**, 282–332.

Rice, S. O. 1945 *Bell. Tech. J.* **24**, 46–156.